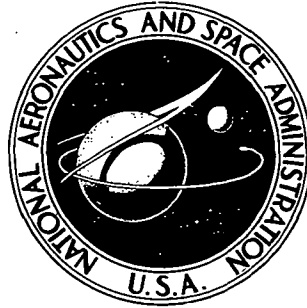


N 72-30777

NASA TECHNICAL NOTE



NASA TN D-6936

NASA TN D-6936

CASE FILE
COPY

SEA-LEVEL EVALUATION
OF DIGITALLY IMPLEMENTED
TURBOJET ENGINE CONTROL FUNCTIONS

*by Dale J. Arpasi, David S. Cwynar,
and Robert E. Wallhagen*

*Lewis Research Center
Cleveland, Ohio 44135*

1. Report No. NASA TN D-6936		2. Government Accession No.		3. Recipient's Catalog No.	
4. Title and Subtitle SEA-LEVEL EVALUATION OF DIGITALLY IMPLEMENTED TURBOJET ENGINE CONTROL FUNCTIONS				5. Report Date September 1972	
				6. Performing Organization Code	
7. Author(s) Dale J. Arpasi, David S. Cwynar, and Robert E. Wallhagen				8. Performing Organization Report No. E-6977	
9. Performing Organization Name and Address Lewis Research Center National Aeronautics and Space Administration Cleveland, Ohio 44135				10. Work Unit No. 764-74	
				11. Contract or Grant No.	
12. Sponsoring Agency Name and Address National Aeronautics and Space Administration Washington, D. C. 20546				13. Type of Report and Period Covered Technical Note	
				14. Sponsoring Agency Code	
15. Supplementary Notes					
16. Abstract The standard hydromechanical control system of a turbojet engine was replaced with a digital control system that implemented the same control laws. A detailed discussion of the digital control system in use with the engine is presented. The engine was operated in a sea-level test stand. The effects of control update interval are defined, and a method for extending this interval by using digital compensation is discussed.					
17. Key Words (Suggested by Author(s)) Digital control Airbreathing propulsion				18. Distribution Statement Unclassified - unlimited	
19. Security Classif. (of this report) Unclassified		20. Security Classif. (of this page) Unclassified		21. No. of Pages 27	
				22. Price* \$3.00	

SEA-LEVEL EVALUATION OF DIGITALLY IMPLEMENTED TURBOJET ENGINE CONTROL FUNCTIONS

by Dale J. Arpasi, David S. Cwynar, and Robert E. Wallhagen

Lewis Research Center

SUMMARY

The standard hydromechanical control system of a turbojet engine was replaced with a digital control system that implemented the same control laws. Three engine variables were controlled. The control required 1227 words of memory and 1.4 milliseconds for calculation. A detailed discussion of the digital control system in use with the engine is presented. The engine was operated in a sea-level test stand.

The response under digital control for update intervals to 25 milliseconds is shown to be comparable to the response under hydromechanical control. At extended update intervals, a deterioration in transient response was noted. The use of digital compensation eliminated most of the response degradation. With compensation, closed-loop transient performance comparable to response under hydromechanical control was achieved at an update interval of 150 milliseconds.

INTRODUCTION

Digital control systems are receiving increased use in aircraft applications. System complexities and interactions require the use of digital controls to obtain optimum performance under all operating conditions. An overall flight control system could include controls for the airframe, the inlets, and the engines operating under the requirements of mission control, navigation, and failure detection systems. Changes in requirements could change not only the performance criteria of the aircraft control systems but also the control laws of these systems to arrive at optimum performance. The use of a digital computer in these flight systems permits maximum interaction and facilitates on-line modifications.

The requirements of the digital computer system necessary to perform the aircraft control functions depend primarily upon the amount of calculation involved and the

dynamics of the systems to be controlled. Being a discrete device, the computer system must be able to sample system measurements, to compute the control functions, and to put out commands at a rate fast enough so as not to impair the required closed-loop transient performance. For a sufficiently complex control law, the necessity of completing the prescribed calculations in the time interval specified by the update rate could lead to the need for very fast and costly computer systems.

This report details the use of a digital computer to control a turbojet engine mounted in a sea-level static stand. The requirements for the digital system necessary to perform this task are indicated. A method is discussed for extending the control update interval to allow more computation time or to permit the use of a slower, less expensive computer to perform the same task.

The digital system performs all functions of the standard hydromechanical control package, with the exception of afterburner control. Transient performance of the engine under digital control is presented for various update intervals. The update interval was extended and the deterioration in transient performance was noted. Digital compensation was incorporated into the measurements of the engine variables and resulted in improved transient performance.

EXPERIMENTAL CONFIGURATION

Digital engine control was carried out on a J85-13 engine operated in a sea-level static test stand. The standard hydromechanical control system of the engine was modified to allow either electronic or hydromechanical computation of any control loop. Overrides, independent of the control, were incorporated to shut down the engine safely if engine overspeed or overtemperature limits are violated or if failures occur in the fuel, hydraulic, or electrical supplies.

Engine Description

The engine is illustrated in figure 1. Inlet air passes through inlet guide vanes into an eight-stage compressor. Air bleed doors are located on the third, fourth, and fifth compressor stages and along with the inlet guide vanes are referred to as the compressor variable geometry. The inlet guide vanes are mechanically coupled to the bleed doors, and the entire compressor variable geometry is driven by mechanically coupled hydraulic actuators located on opposite sides of the engine. The compressor variable geometry servomechanism control loop is scheduled to optimize compressor performance over its complete range of operation.

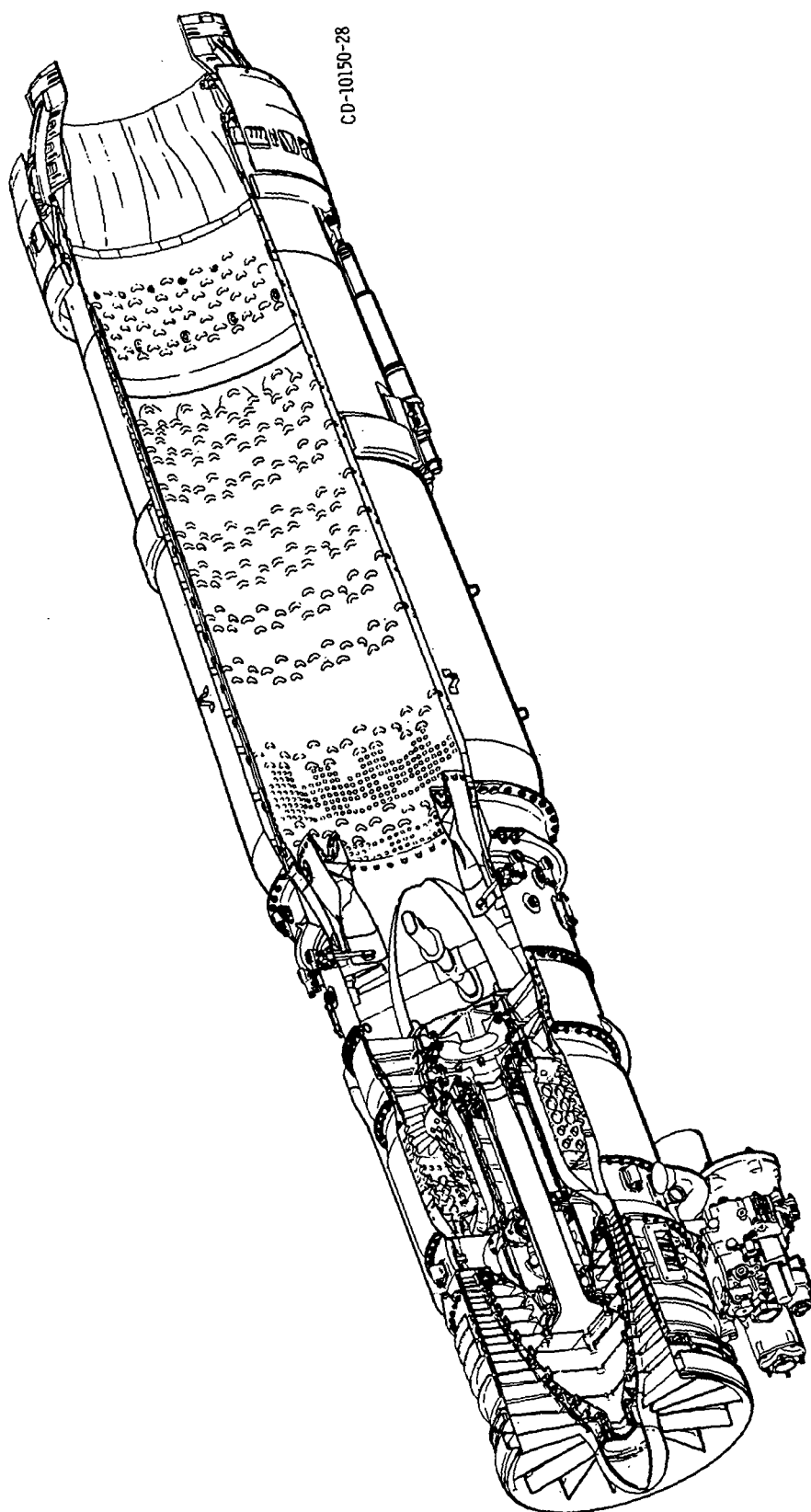


Figure 1. - Cutaway view of J85 engine.

A fuel control regulates fuel flow into the burner. The fuel flow passes through a pressurizing and drain valve and an overspeed governor before it enters the burner spray bars. The fuel and compressor variable geometry controls are located together in one of two hydromechanical packages located beneath the engine.

Control of the variable exhaust nozzle area is provided by the other hydromechanical package. The output of this control is a mechanical position used to command three linear translating mechanical actuators coupled to the exhaust nozzle unison ring. Motion of the unison ring moves the nozzle leaves, thus varying nozzle throat area.

Modification for Digital Control

The standard hydromechanical engine control system was modified to permit selective substitution of digital control for the standard hydromechanical controls of compressor variable geometry, fuel, and variable nozzle area and to permit easy switching between the two (for safety reasons). Hydromechanical computation of each control schedule was maintained, except for the compressor variable geometry. The hydraulic output from the standard hydromechanical control normally used to drive the compressor variable geometry actuators was inactivated. The compressor variable geometry schedule was implemented on a special-purpose analog computer.

A block diagram of the experimental configuration is shown in figure 2. A servo-amplifier, of the type described in reference 1, was used to drive a servovalve to form the compressor variable geometry position loop. The servovalve powered the standard actuators; and their position, as measured by an engine-mounted linear potentiometer, was fed back to the servoamplifier to close the position loop. The command to the compressor variable geometry servoamplifier could be switched from either the analog computer schedule or the digital schedule.

The main fuel control was left intact, with the exception of a four-way switching valve which was inserted in the engine fuel supply line just ahead of the overspeed governor. This allowed manual switching of engine fuel flow between the hydromechanical control and the digital control. The digital command scheduled the output of a fast-response fuel metering device (ref. 2) whose output was sent to the four-way switching valve. The selected fuel was ported by the valve to the engine while the unselected fuel was ported to drain through a dummy load.

The standard exhaust nozzle control determines the position of a mechanical arm located on the exhaust nozzle control package. This arm is normally used to drive a power pack which in turn drives mechanical screw-jack actuators attached to the nozzle leaves through a unison ring. This system was modified by replacing the mechanical screw-jack actuators with hydraulic actuators and closing a servomechanism control

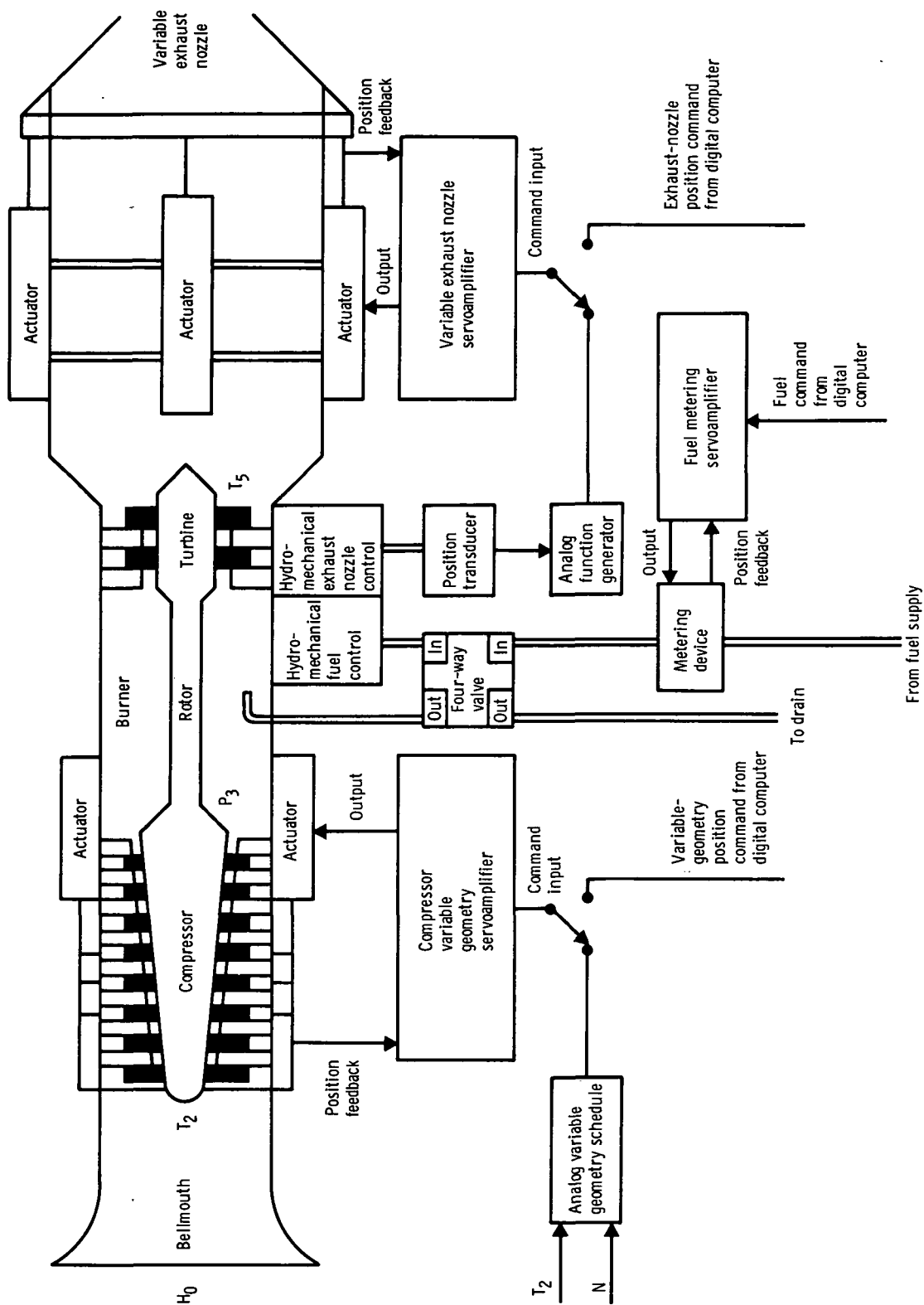


Figure 2. - Modifications to standard hydromechanical control system to permit switching to digital control system.

loop around them in the same way as described for the compressor variable geometry control. The power pack was removed, and a linear displacement transducer was installed to measure the position of the mechanical arm. The transducer output was scaled and linearized by an analog function generator so that the proper unison ring position command was presented to the exhaust nozzle servoamplifier. The command to the exhaust nozzle servoamplifier could be switched from either the analog function generator or the digital schedule.

Signal conditioners were used to provide high-level signals (-10 V to +10 V) from the transducer measurements. Throttle position α was measured by attaching a rotating potentiometer to the shaft of the throttle input to the hydromechanical fuel control. A static pressure tap attached to a high-response gage transducer was used to provide compressor discharge pressure P_3 measurement. Engine speed N was measured by attaching a special gear to the engine power-takeoff and counting gear teeth with a magnetic pickup. The resultant frequency was converted to dc before being routed to the digital system. Thermocouples were used for measurement of both compressor inlet temperature T_2 and turbine exit temperature T_5 . An absolute pressure transducer was used to provide an ambient pressure H_0 measurement for use in correcting P_3 to absolute.

The digital system ground was isolated from the experiment through isolation amplifiers. This eliminated the possibility of ground loops and provided relatively noise-free measurements.

CONTROL FUNCTIONS AND DIGITAL IMPLEMENTATION

A block diagram of the digital system is given in figure 3. It consists of a signal processing unit, an interface unit, a digital computer, and programming peripherals. The signal processing unit provides isolation of the signal inputs and calibration of the interface unit. The interface unit contains a high-level multiplexer, a single sample-and-hold amplifier, and a 13-bit digitizer to provide analog-to-digital conversion of the six measured signals. Digital-to-analog conversion of the computer commands is also accomplished in the interface through 13-bit digital-to-analog conversion units. The analog commands for compressor variable geometry position X_{vg} , fuel flow W_f , and exhaust nozzle area A_8 are obtained through separate digital-to-analog converters.

The computer itself is a 16-bit machine with 16 384 words of magnetic core storage. The read-restore cycle time of the memory is 750 nanoseconds. Programming of the computer is done through a teletype and high-speed paper tape reader and punch. All control programming was done in assembly language to conserve core storage and execution time.

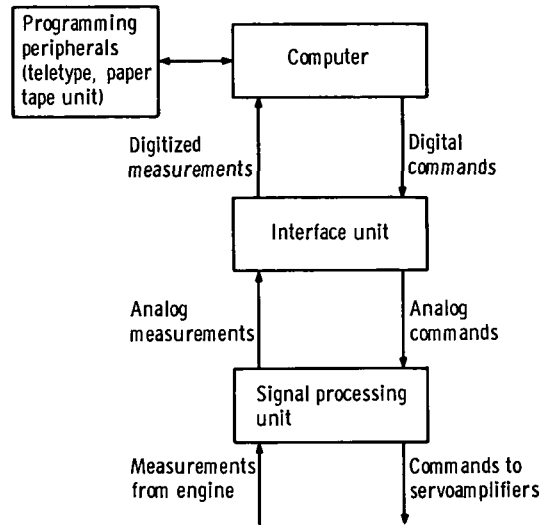


Figure 3. - Block diagram of digital control system.

A complete description of this general-purpose digital system is given in reference 3. Pertinent specifications of the signal processing unit, the interface units, and the computer are presented in table I.

Compressor Variable Geometry Control

The compressor variable geometry control schedules position X_{vg} as a function of corrected rotor speed $N/\sqrt{\theta}$ and compressor inlet temperature T_2 . In general, as $N/\sqrt{\theta}$ increases, the compressor variable geometry is scheduled to close. Increasing T_2 causes the variable geometry to open. The variable geometry includes the inlet guide vanes and the bleed doors. This control function was implemented on the digital computer by storing three curves of X_{vg} against $N/\sqrt{\theta}$ (each at constant T_2) in memory. Linear interpolation was used to compute X_{vg} as a function of $N/\sqrt{\theta}$ and also to interpolate between lines of constant T_2 .

Fuel Control

The fuel control commands a required ratio of fuel flow to static compressor discharge pressure W_f/P_3 as a function of throttle position α , engine speed N , and compressor inlet temperature T_2 . The ratio is multiplied by the measured P_3 , resulting in the required fuel flow.

TABLE I. - DIGITAL SYSTEM CAPABILITIES

Digital computer	
Magnetic core memory size, words	16 384
Word length, bits plus parity	16
Memory cycle time, nsec	750
Add time, μ sec	1.5
Subtract time, μ sec	1.5
Multiply time, μ sec	4.5
Divide time, μ sec	8.25
Load time, μ sec	1.5
Store time, μ sec	1.5
Indirect addressing	Infinite
Indexing	Total memory
Priority interrupts	28 Separate levels
Index registers:	
Independent	1
In conjunction with lower accumulator	1
Physical size, in. :	
Width	24
Height	62
Depth	30
Interval timers	
Complement	2
Accuracy, clock pulses	± 1
Clock rates, kHz	572, 286, 160, 143, 80, 71.5, 40, 35.75, 20, 10
Counter	16-Bit binary
Output	Priority interrupt to computer
Analog acquisition unit	
Overall sample rate (maximum), kHz	20
Resolution of digital data, bits	12 (plus sign)
Output code	Two's complement
Number of channels	64
Input range, V full scale	± 10
Input impedance, $M\Omega$ (shunted by 10 pF)	10
Maximum source resistance, Ω	1000
Conversion time, μ sec	38
Input setting time, μ sec	9
Sample-and-hold aperture time, nsec	500
Safe input voltages, V	± 20 sustained ± 100 for less than 100 μ sec
Total error with calibration, percent	0.073

TABLE I. - Concluded. DIGITAL SYSTEM CAPABILITIES

Frequency acquisition unit	
Number of channels	10
Nature of input	Continuously varying or pulsatile
Resolution of digital data, bits	12
Switch selectable clock rates, kHz	20, 80, 100, 400, external
Overall accuracy, bits	± 1
Update rate	Once per cycle of input frequency
Maximum input frequency, kHz	1
Input amplitude range	100 mV to 30 V peak to peak
Analog output unit	
Total number of digital-to-analog conversion channels	26
Resolution (10 channels), bits	12 (plus sign)
Resolution (16 channels), bits	11 (plus sign)
Output voltage range, V full scale	± 10
Output current (maximum), mA	10
Output impedance, Ω	< 1
Accuracy (12 bit), percent of full scale	± 0.1
Accuracy (13 bit), percent of full scale	± 0.05
Slew rate, V/ μ sec	1
Settling time for 10-V step to within 0.05 percent of final value, μ sec	20
Logical output unit	
Number of electronic switch outputs	32
Number of contact closure outputs	32
Maximum voltage, V	30
Maximum current, mA	100
Priority interrupt processor	
Number of channels	10
Input impedance, $k\Omega$	47
Input voltage range, V	± 10
Comparator switching	Trigger on rise or fall
Comparator hysteresis	Adjustable from 35 mV to 650 mV
Comparator output, V	$+7$
Monostable multivibrator:	
Pulse width, μ sec	.3
Pulse height, V	$+7$

A typical operating map of W_f/P_3 against $N/\sqrt{\theta}$ is shown in figure 4. Droop lines (lines of constant α) are shown intersecting a normal steady-state operating line. A change in α , from α_1 to α_2 , at constant $N/\sqrt{\theta}$ causes a step in W_f/P_3 . The W_f/P_3 command is limited by the acceleration schedules, which are functions of T_2 . As N increases, the W_f/P_3 command follows the proper acceleration schedule until it intersects the α_2 droop line, which it then follows to its steady-state value. The acceleration schedules are shaped to avoid turbine overtemperature and compressor stall during acceleration.

In the droop-line calculation on the digital computer, desired steady-state values of W_f/P_3 and N were computed as functions of α and T_2 . Actual engine speed was subtracted from the desired speed to form a speed error. This error was multiplied by a proportional gain and added to the desired W_f/P_3 value to form the desired droop-line output, $(W_f/P_3)_d$. The gain was proportional to N , giving the parabolic shape to the droop lines.

In order to generate the acceleration schedules on the digital computer, eight curves of W_f/P_3 against $N/\sqrt{\theta}$ at constant T_2 were stored in the computer memory. The measured T_2 was compared to each of the eight values until the immediately lower value, T_{min} , and the immediately higher value, T_{max} , were found. Linear interpolation was used to find the W_f/P_3 value corresponding to $N/\sqrt{\theta}$ at T_{min} and T_{max} . Linear interpolation was again used between these values to find the acceleration limit.

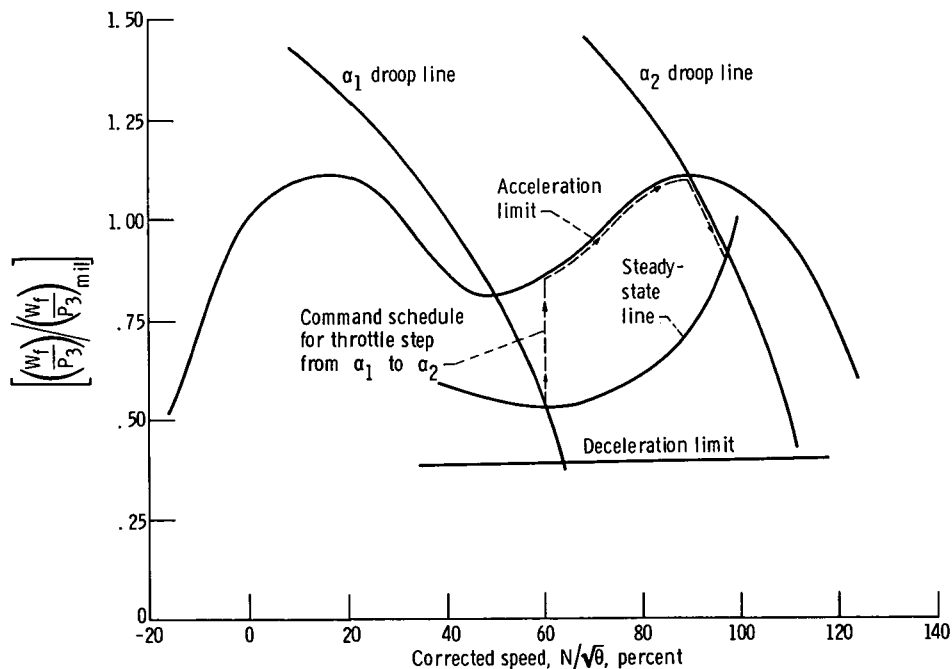


Figure 4. - Typical engine fuel control operating map showing acceleration and deceleration limits.

value, $(W_f/P_3)_a$, corresponding to the measured T_2 .

Upon completion of the droop and acceleration calculations, the smaller of $(W_f/P_3)_d$ and $(W_f/P_3)_a$ was selected. If the acceleration limit was chosen, a logic indicator V_s was set as an acceleration indication to the exhaust nozzle control. A minimum limit on W_f/P_3 was incorporated to provide a deceleration schedule. The result was then multiplied by the measured P_3 to form the fuel-flow command. This command had a minimum limit at a value of fuel flow necessary to sustain combustion. For engine shutdown, a function was included which commanded zero fuel flow as the throttle was completely retarded.

Exhaust Nozzle Area Control

The exhaust nozzle area A_8 was controlled primarily as a function of α . Certain engine conditions caused an override of the throttle-commanded area. If the engine was operating on the fuel control's acceleration limit (V_s set), the minimum area was made equal to a fixed area, A_{8a} , to allow faster acceleration. At low compressor discharge pressure the area was also limited from closing to less than a function of P_3 , A_{8p} , to provide compressor stall protection.

The exhaust nozzle control also provides turbine overtemperature protection by overriding the normal throttle-scheduled area with an integral-proportional regulation of turbine exhaust gas temperature T_5 . This regulation was implemented on the digital computer by taking the Z-transform of the control function used in the standard hydro-mechanical control. The resultant T_5 override area A_{8t} was limited to its full-closed value whenever T_5 was less than its reference value. A maximum selector was used to pick the larger of the normal area command or A_{8t} . Consequently, if T_5 exceeded its reference value, the nozzle would open and reduce T_5 . The reference value was made a function of a nominal T_5 limit, T_2 , and N .

Input-Output and Timing

The three controls (compressor variable geometry, fuel, and exhaust nozzle), implemented as described, require the measurement of six variables - α , N , T_2 , T_5 , P_3 , and H_0 . A high-level (-10 V to +10 V) multiplexer, a sample-and-hold, and a digitizer under block data transfer control (ref. 3) were used to take sampled values of these measurements directly into computer memory on a cycle-stealing basis. That is, upon computer command, channel transfer to the multiplexer and data transfer from the

digitizer were accomplished automatically without interrupting the computer for more than one memory cycle per word transferred. The sample-hold-digitizing processes operated at a rate of 20 000 words per second ($50 \mu\text{sec}/\text{word}$). Acquisition of the six measured variables, therefore, required 300 microseconds. A priority interrupt was issued by the block transfer control to the computer when all six words were in memory.

A 13-bit digital-to-analog converter was assigned to each of the control outputs (X_{vg} , W_f , and A_8). Upon completion of the control computation, these commands were issued from the computer and required 6.75 microseconds per word transferred.

A timing diagram giving the event sequence over an update interval ΔT is presented in figure 5. The control process was sequenced through the use of an interval timer.

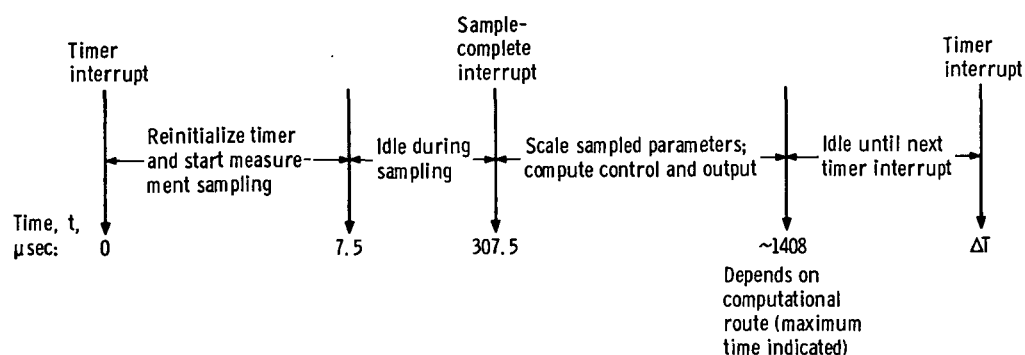


Figure 5. - Timing diagram for typical update interval.

This timer accepts a digital word from the computer and counts it down at a fixed rate. When the countdown reaches zero, the timer issues a priority interrupt to the computer, indicating that a fixed amount of time has elapsed. The magnitude of the word dictates the length of the update interval ΔT . Upon receiving the timer interrupt, the computer reinitializes the timer for the next update interval and begins sampling the six measured variables and taking the digitized values into assigned memory locations. This requires about 7.5 microseconds. The computer then idles for 300 microseconds during the digitizing period. During idle periods, the computer is available for processing other routines if so required.

When the measurements are in memory, the priority interrupt from the block data transfer control occurs and the control computation begins. This computation time depends on the route taken through the program and averages about 1.1 milliseconds. Upon completion of the computation the manipulated variables are updated and the computer idles until the next priority interrupt from the interval timer.

Calculation times and memory requirements for each subroutine and the complete control calculation are presented in table II. This table provides time information in

TABLE II. - CONTROL COMPUTATION MEMORY AND TIMING REQUIREMENTS

[Control calculation plus sample time, 1.4 msec.]

Routine name	Routine function	Memory words required	Memory cycles required		Computation ^a time, msec	
			Minimum	Maximum	Minimum	Maximum
CSPEED	Compute corrected speed ($N/\sqrt{\theta}$)	28	29 + FG	29 + FG	0.022 + FG	0.022 + FG
FG	Linear interpolation function generation	26	64	64	0.048	0.048
VG	Compute variable geometry control	114	12	71 + 2FG	0.009	0.053 + 2FG
MFC	Compute fuel control	40	50 + DROOP + ACCEL	57 + DROOP + ACCEL	0.038 + DROOP + ACCEL	0.043 + DROOP + ACCEL
DROOP	Compute location on droop line	62	85 + MCAM + TCOM	101 + MCAM + TCOM	0.064 + MCAM + TCOM	0.075 + MCAM + TCOM
MCAM	Compute steady-state W_F/P_3 commands	88	17	26 + 2FG	0.013	0.02 + 2FG
TCOM	Compute temperature compensation	74	20 + FG	31 + FG	0.015 + FG	0.023 + FG
ACCEL	Compute acceleration limit	365	87 + 2FG	129 + 2FG	0.065 + 2FG	0.097 + 2FG
VEN	Compute variable exhaust nozzle control	183	127	251	0.095	0.188
MAIN (1)	Program initialization	68	(b)	(b)	(b)	(b)
MAIN (2)	Timer control, data acquisition control, scaling and calling of control subroutines	179	260	260	0.196	0.196
Total control calculation		1227	943	1467	0.71	1.1

^aBased on memory cycle time of 750 nsec.^bExecuted only once upon program start.

terms of memory cycles (to allow the reader to estimate calculation time for other computers) and in terms of milliseconds based on the computer used in this experiment. The complete engine control program requires 1227 words of memory and a maximum of 1.4 milliseconds of time including sampling. The maximum calculation time is based on manufacturer published times for the computer instruction set.

RESULTS AND DISCUSSION

The control update interval ΔT determines how often the engine variables are sampled and how often the commands are updated. The minimum possible ΔT is set by the sum of the sampling time and calculation time of the digital system. Table II indicates that for this system the maximum calculation time is 1.15 milliseconds and the time necessary to sample the six measured variables is 0.3 millisecond. The minimum ΔT possible with this control is, therefore, 1.5 milliseconds.

Engine transient response dictates the maximum possible update interval. Since the engine is a nonlinear device, it would not suffice to evaluate the effects of increased ΔT by using linear stability analysis at a single operating point. For this reason, throttle position steps from idle (approx. 50-percent N) to military (100-percent N) were used to provide the engine transients for update interval evaluation purposes.

The dashed lines in figure 6 illustrate the engine response under the modified hydro-

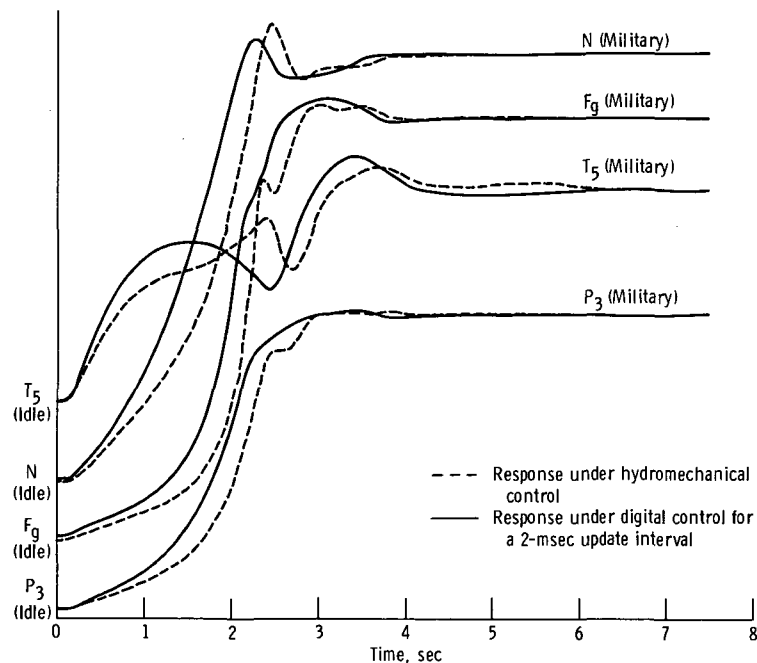


Figure 6. - Comparison of digital and hydromechanical controls for a throttle step from idle to military.

mechanical control (fig. 2) for a throttle slam from idle to military. Hereinafter, the modified hydromechanical control of figure 2 will be referred to simply as the hydromechanical control. Rotor speed N , turbine discharge temperature T_5 , compressor exit static pressure P_3 , and gross thrust F_g are plotted against time. The same figure gives the response of the engine under digital control (solid lines) for an update interval ΔT of 2 milliseconds. The digital response does not exactly match the modified hydromechanical response. It exhibits a somewhat shorter rise time and less overshoot in rotor speed, while allowing more overshoot in turbine exhaust gas temperature. These differences were traced to slight schedule differences in the main-fuel and variable exhaust nozzle control systems. The digital schedules were taken from and checked against information received from the manufacturer.

Figure 7 is a plot of compressor pressure ratio against corrected speed during the same throttle slam from idle to military. The response under hydromechanical control is approximately equivalent to the response under digital control. The apparent discrepancy at the high end of the transient is due to differences in the exhaust nozzle control. Under hydromechanical control the nozzle closes earlier, causing a faster rise in pressure ratio and increased overshoot in corrected speed.

The response of the engine to the large-scale transients may be evaluated in terms

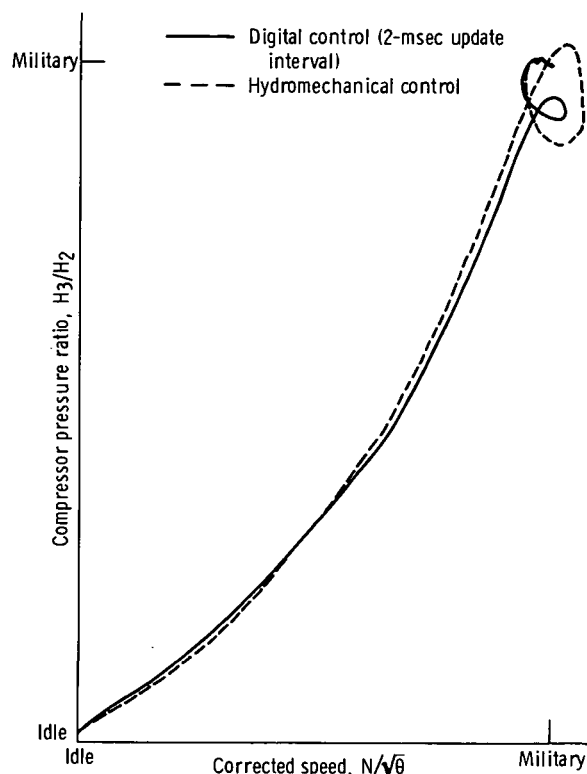


Figure 7. - Effect of digital and hydromechanical controls on compressor pressure ratio for a throttle step from idle to military.

of the time required to move from one operating level to another and how well it remained within the prescribed operating limits of the engine. These limits are engine overspeed, turbine overtemperature, compressor stall, and blade vibrations. The engine was not instrumented to measure blade vibrations. However, engine vibration was monitored by panel meters and was well within prescribed limits for all conditions discussed in this report. The engine response under the modified hydromechanical control was used to provide a conservative estimate of the operational limits.

Comparisons of the responses in figures 6 and 7 illustrate that under digital control at the 2-millisecond update interval the engine response equals or surpasses the response under hydromechanical control. The possible exception is the turbine exhaust gas temperature overshoot. This overshoot is a function of the integral and proportional gains in the T_5 override of the variable exhaust nozzle control; it could have been trimmed to exactly match the hydromechanical characteristics. However, since the real temperature limit is that of the turbine blades, this slight overshoot in gas temperature was considered negligible.

Effects of Control Update Interval

The effects of update interval on engine response are shown in figures 8 and 9, for

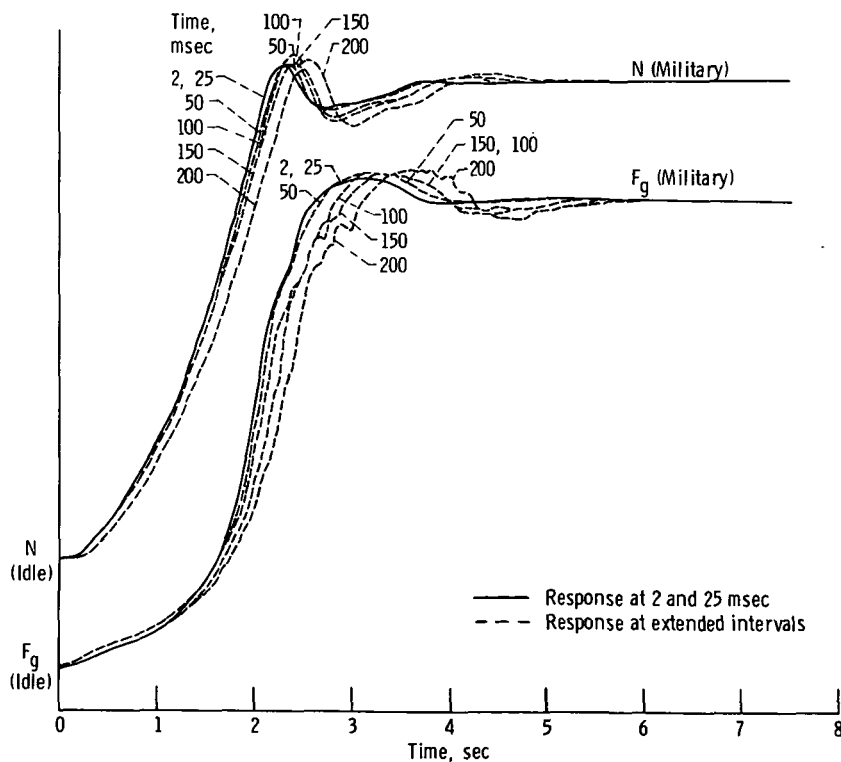


Figure 8. - Effects of update interval on engine response for a throttle step from idle to military.

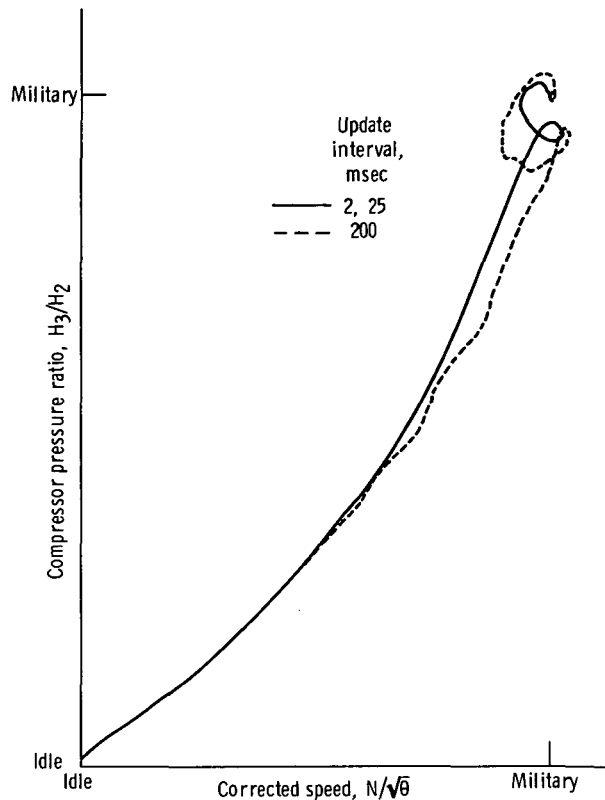


Figure 9. - Effect of update interval on compressor pressure ratio for a throttle step from idle to military.

update intervals of 2, 25, 50, 100, 150, and 200 milliseconds. For simplification purposes, only gross thrust and rotor speed are illustrated in figure 8 and only the 2-, 25-, and 200-millisecond intervals are illustrated in figure 9. The engine response was stable throughout this range. However, as the update interval was increased, the engine response deteriorated in terms of rise time; and between 25 and 50 milliseconds the overshoot in rotor speed exceeded the 2-millisecond reference response. Figure 9 indicates that the pressure ratio transient response at a ΔT of 200 milliseconds did not appreciably exceed the 2-millisecond reference response.

From the data of figures 8 and 9, it can be stated that the digital control with a ΔT of 25 milliseconds was indistinguishable from the control with a ΔT of 2 milliseconds. At extended intervals the response deteriorated (although not extremely), and violation of the engine operational limits was possible.

Use of Digital Compensation to Extend Update Interval

The deterioration in response with increased update interval is due to the fact that

the sampled values of the measurements at the start of an interval are an increasingly poor approximation to the values of the variables over the interval. The value of a variable in the n^{th} time interval $e_n(t)$ can be approximated by a power series (ref. 4) of the form

$$e_n(t) = e(n \Delta T) + \dot{e}(n \Delta T)(t - n \Delta T) + \frac{1}{2!} \ddot{e}(n \Delta T)(t - n \Delta T)^2 + \dots \quad (1)$$

where $e(n \Delta T)$ is the sampled value of the variable at time $n \Delta T$, and \dot{e} and \ddot{e} are the first and second derivatives, respectively. (All symbols are defined in the appendix.) Time t goes from $n \Delta T$ to $(n + 1)\Delta T$. If ΔT is appreciable and the measured variable is changing rapidly, much information on the state of the variable is missing from the sampled value.

The deterioration in response with increased ΔT can be further explained by studying the frequency response of a digital sampler and zero-order hold shown in figure 10. The frequency axis is shown as a function of the sampling frequency $f_s = 1/(\Delta T)$.

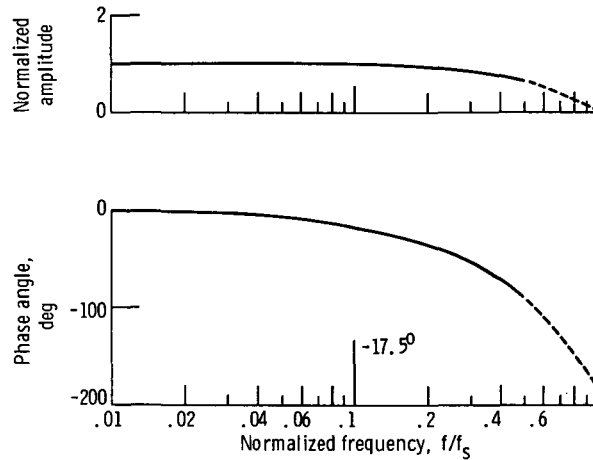


Figure 10. - Normalized frequency response of a sample-and-hold. $G(s) = (1 - e^{-\Delta T s})/\Delta T s$.

As long as f_s is large compared to the engine frequencies f , the sample-and-hold adds little to the closed-loop dynamics (amplitude ≥ 0.98 , phase $\geq -17.5^\circ$). Decreasing f_s (increasing f/f_s beyond 0.1), however, introduces appreciable attenuation and phase shift. If we could compensate for this attenuation and phase shift, we could extend the update interval (decrease f_s) while maintaining good engine response.

A typical sample-and-hold-compensation operation is depicted in the block diagram of figure 11. The variable e_m is any engine variable sampled and held to produce the discrete variable e_h . Digital compensation of e_h results in the discrete variable e_c .

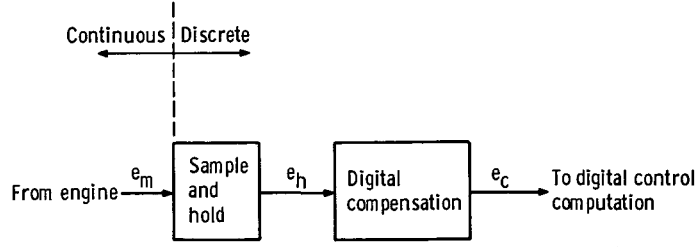


Figure 11. - Block diagram of digitally compensated sample-and-hold of a typical engine variable.

In an effort to provide some phase lead, the compensator was made to be a linear function of the digital estimations to the first and second derivatives of e_h and is given by

$$e_c(n \Delta T) = e_h(n \Delta T) + K_1 \Delta T \dot{e}_h(n \Delta T) + K_2 \Delta T^2 \ddot{e}_h(n \Delta T) \quad (2)$$

The derivative gains K_1 and K_2 were variable and adjusted experimentally to improve the engine response to throttle steps.

The digital estimations of derivatives are

$$\dot{e}_h(n \Delta T) = \frac{1}{\Delta T} \{e_h(n \Delta T) - e_h[(n-1)\Delta T]\} \quad (3)$$

$$\ddot{e}_h(n \Delta T) = \frac{1}{(\Delta T)^2} \{e_h(n \Delta T) - 2e_h[(n-1)\Delta T] + e_h[(n-2)\Delta T]\} \quad (4)$$

Substituting equations (3) and (4) into equation (2) produces the digital equation

$$e_c(n \Delta T) = (1 + K_1 + K_2)e_h(n \Delta T) - (K_1 + 2K_2)e_h[(n-1)\Delta T] + K_2e_h[(n-2)\Delta T] \quad (5)$$

In order to observe the effects of compensation in the frequency domain, equation (5) may be rewritten in Laplace transform notation as

$$\frac{e_c(s)}{e_h(s)} = (1 + K_1 + K_2) - (K_1 + 2K_2)e^{-\Delta Ts} + K_2e^{-2\Delta Ts} \quad (6)$$

The net result of including this digital compensation is given by the transfer function

$$\frac{e_c(s)}{e_m(s)} = \frac{1 - e^{-\Delta T s}}{\Delta T s} \left[(1 + K_1 + K_2) - (K_1 + 2K_2)e^{-\Delta T s} + K_2 e^{-2\Delta T s} \right] \quad (7)$$

A frequency domain plot of this transfer function is shown in figure 12 for $K_1 = 1$ and $K_2 = 0.5$. When this response is compared to that of the uncompensated sample-and-hold shown in figure 10, the large amount of phase lead added by the compensation becomes apparent. However, it should also be noted that substantial gain is also inserted

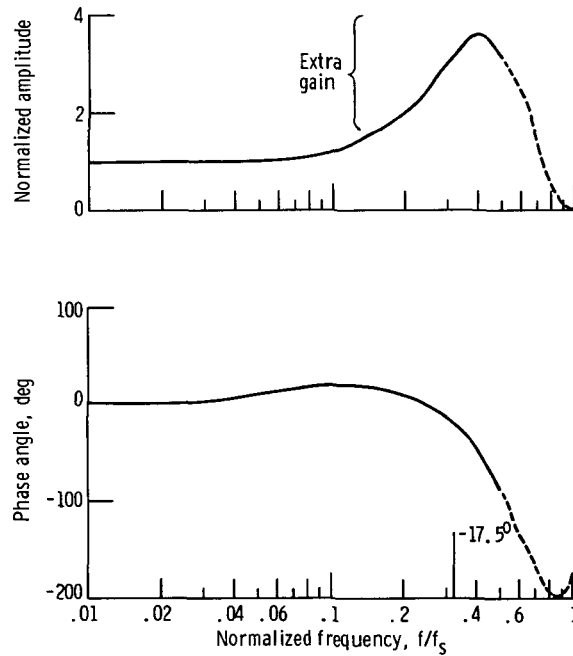


Figure 12. - Normalized frequency response of a compensated sample-and-hold. $G(s) = \frac{[1 - e^{-\Delta T s}]/\Delta T s}{(2.5 - 2e^{-\Delta T s} + 0.5e^{-2\Delta T s})}$.

into the control loop by the compensation, which tends to reduce the stability margin of the closed loop.

To demonstrate the effects of this type of compensation on the engine at extended update intervals, the relation given by equation (5) was programmed into the measurement of N , P_3 , and T_5 . That is, each of these variables was sampled and held as before, but before being acted upon by the control program they were each compensated according to equation (5). The amount of compensation (K_1 and K_2) was increased from zero at a ΔT of 150 milliseconds and the response of the engine to throttle slams was observed.

An example of the effects of compensation on the engine response to throttle slams

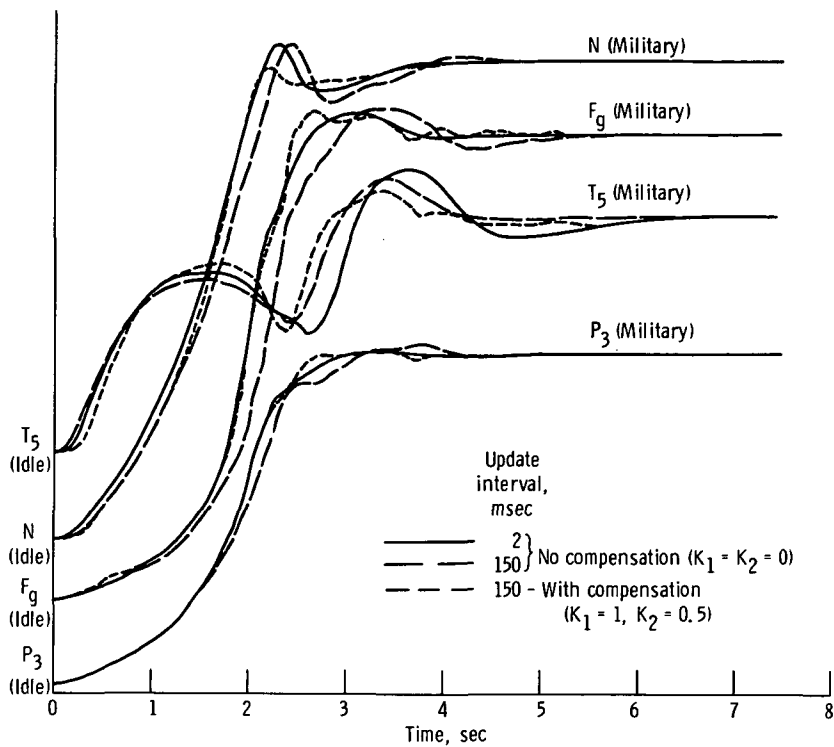


Figure 13. - Effects of compensation on engine response for a throttle step from idle to military.

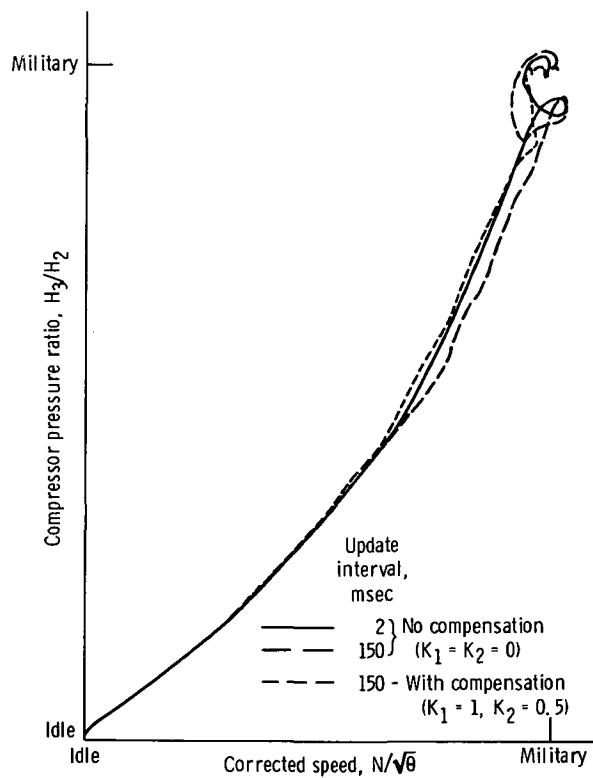


Figure 14. - Effects of compensation on compressor pressure ratio for a throttle step from idle to military.

is given in figures 13 and 14. The sampled values of N , P_3 , and T_5 were compensated according to the equations

$$N_c(n \Delta T) = 2.5N_h(n \Delta T) - 2N_h[(n-1)\Delta T] + 0.5N_h[(n-2)\Delta T] \quad (8)$$

$$P_{3c}(n \Delta T) = 2.5P_{3h}(n \Delta T) - 2P_{3h}[(n-1)\Delta T] + 0.5P_{3h}[(n-2)\Delta T] \quad (9)$$

$$T_{5c}(n \Delta T) = 2.5T_{5h}(n \Delta T) - 2T_{5h}[(n-1)\Delta T] + 0.5T_{5h}[(n-2)\Delta T] \quad (10)$$

For comparison purposes the engine responses without compensation at update intervals of 2 milliseconds and 150 milliseconds are also shown in this figure. The use of compensation essentially allowed the response at 150 milliseconds to match the uncompensated response at 2 milliseconds. It was found, however, that any further increases in the derivative gains K_1 and K_2 resulted in instability at high-rotor-speed operation. This instability was manifested in terms of diverging oscillations in fuel flow. It was also determined that the response with this compensation was very sensitive to changes in compressor inlet temperature T_2 (T_2 for figs. 13 and 14 was approximately 311 K (100° F) at military operation). Unfortunately, documentation of the effects of temperature was not possible because of the inability to regulate this variable in the test facility.

It should be remembered that responses for sampling intervals up to 25 milliseconds were essentially equivalent to that at 2 milliseconds. Therefore, operation at 150 milliseconds as opposed to 2 milliseconds results in an increase in computer efficiency of 6 to 1. At 150 milliseconds only 1/100th of the interval is being used in the control computation. The remainder of the time may be used to provide other aircraft control and monitoring services. In another regard, the use of compensation allows the use of slower and less expensive computing hardware while maintaining the response of a fast machine. The compensation described is by no means optimum or unique but indicates the advantages of the use of digital compensation in aircraft control applications.

CONCLUSIONS

A digital control system to replace the hydromechanical control of compressor variable geometry, main fuel flow, and variable exhaust nozzle area of a J85-13 turbojet engine requires a computer with slightly less than 1500 words of core storage. The entire digital control process can be calculated in approximately 1500 computer memory cycles. The repetitive update interval may be extended to 25 milliseconds without appreciable degradation in closed-loop response.

Digital compensation, making use of weighted approximations to the derivatives to incorporate prediction into the sampled engine variables, allows extension of the maximum update interval to 150 milliseconds with no appreciable loss in engine response.

Lewis Research Center,
National Aeronautics and Space Administration,
Cleveland, Ohio, June 12, 1972,
764-74.

APPENDIX - SYMBOLS

A_8	exhaust nozzle area, cm^2
A_{8a}	exhaust nozzle area during acceleration, cm^2
A_{8p}	exhaust nozzle area as function of pressure, cm^2
A_{8t}	exhaust nozzle area as function of temperature, cm^2
e	any engine variable
\dot{e}	first time derivative of e
\ddot{e}	second time derivative of e
F_g	gross thrust, N
f	frequency, Hz
f_s	sampling frequency, Hz
G	transfer function (appropriate dimensions)
H_0	ambient total pressure, N/cm^2
H_2	compressor inlet total pressure, N/cm^2
H_3	compressor exit total pressure, N/cm^2
K_1	first derivative gain, dimensionless
K_2	second derivative gain, dimensionless
N	percent rotor speed
$N/\sqrt{\theta}$	percent corrected rotor speed
n	integer
P_3	compressor discharge static pressure, N/cm^2
s	Laplace variable, sec^{-1}
T	temperature, K
T_2	compressor inlet temperature, K
T_5	turbine exhaust temperature, K
ΔT	sampling interval, sec
t	time, sec
V_s	logic indicator
W_f	fuel flow, kg/hr

X_{vg} variable geometry position, percent
 α throttle position, deg
 ϵ exponential function

Subscripts:

a acceleration
c digital compensator output
d droop
h sample-and-hold output
m measured
max maximum
mil military
min minimum

REFERENCES

1. Zeller, John R.: Design and Analysis of a Modular Servoamplifier for Fast-Response Electrohydraulic Control Systems. NASA TN D-4898, 1968.
2. Batterton, Peter G.; and Zeller, John R.: Dynamic Performance Analysis of a Fuel-Control Valve for Use in Airbreathing Engine Research. NASA TN D-5331, 1969.
3. Arpasi, Dale J.; Zeller, John R.; and Batterton, Peter G.: A General Purpose Digital System for On-Line Control of Airbreathing Propulsion Systems. NASA TM X-2168, 1971.
4. Kuo, Benjamin C.: Analysis and Synthesis of Sampled-Data Control Systems. Prentice-Hall, Inc., 1963.



POSTMASTER: If Undeliverable (Section 158
Postal Manual) Do Not Return

"The aeronautical and space activities of the United States shall be conducted so as to contribute . . . to the expansion of human knowledge of phenomena in the atmosphere and space. The Administration shall provide for the widest practicable and appropriate dissemination of information concerning its activities and the results thereof."

— NATIONAL AERONAUTICS AND SPACE ACT OF 1958

NASA SCIENTIFIC AND TECHNICAL PUBLICATIONS

TECHNICAL REPORTS: Scientific and technical information considered important, complete, and a lasting contribution to existing knowledge.

TECHNICAL NOTES: Information less broad in scope but nevertheless of importance as a contribution to existing knowledge.

TECHNICAL MEMORANDUMS: Information receiving limited distribution because of preliminary data, security classification, or other reasons.

CONTRACTOR REPORTS: Scientific and technical information generated under a NASA contract or grant and considered an important contribution to existing knowledge.

TECHNICAL TRANSLATIONS: Information published in a foreign language considered to merit NASA distribution in English.

SPECIAL PUBLICATIONS: Information derived from or of value to NASA activities. Publications include conference proceedings, monographs, data compilations, handbooks, sourcebooks, and special bibliographies.

TECHNOLOGY UTILIZATION PUBLICATIONS: Information on technology used by NASA that may be of particular interest in commercial and other non-aerospace applications. Publications include Tech Briefs, Technology Utilization Reports and Technology Surveys.

Details on the availability of these publications may be obtained from:

**SCIENTIFIC AND TECHNICAL INFORMATION OFFICE
NATIONAL AERONAUTICS AND SPACE ADMINISTRATION
Washington, D.C. 20546**